International Journal of Mechanical, Industrial and Aerospace Sciences
ISSN: 2517-9950
Vol:4, No:10, 2010

Particle Simulation of Rarefied Gas Flows with a Superimposed Wall Surface Temperature Gradient in Microgeometries

V. Azadeh Ranjbar

Abstract**—**Rarefied gas flows are often occurred in micro electro mechanical systems and classical CFD could not precisely anticipate the flow and thermal behavior due to the high Knudsen number. Therefore, the heat transfer and the fluid dynamics characteristics of rarefied gas flows in both a two-dimensional simple microchannel and geometry similar to single Knudsen compressor have been investigated with a goal of increasing performance of a actual Knudsen compressor by using a particle simulation method. Thermal transpiration and thermal creep, which are rarefied gas dynamic phenomena, that cause movement of the flow from less to higher temperature is generated by using two different longitude temperature gradients (Linear, Step) along the walls of the flow microchannel. In this study the influence of amount of temperature gradient and governing pressure in various Knudsen numbers and length-to-height ratios have been examined.

Keywords**—**DSMC, Thermal transpiration, Thermal creep, MEMS, Knudsen Compressor.

I. INTRODUCTION

GAS flows at micro scale have recently gained intensive attention due to the rapidly developed micro electro mechanical devices [1]. Study of these flows is important for both fundamental scientific issues and technological applications. To enhance the design and performance of micro electro mechanical systems, it is necessary to achieve deeper understanding of the related flow and thermal behaviors [2].

In most microflows, the mean free path of the fluid, λ, is of the same order as the system characteristic length. So the Knudsen number, which is the ratio of the two lengths, can be quite high even when the fluid is dense. Therefore the continuum assumption breaks down. Also in some micro devices under temperature gradient like Knudsen compressor, gas flows are frequently significant non-equilibrium because of rarefaction effect. Consequently the constitutive relations for the stress tensor and the heat flux vector, in terms of macroscopic parameters (bulk velocity, density, temperature) that appear in the Navier-Stokes equations, break down.

So modeling of microflows with difficult boundary conditions and non-equilibrium state should be based on a molecular point of view since traditional CFD techniques applied to microflow analyses may lead to large errors.

The direct simulation Monte Carlo method (DSMC) [3, 4, 5 and 6] is one of the best methods for modeling such microchannel flows that have been used [7, 8 and 9]. The DSMC method avoids solving the Boltzmann equation mathematically and by tracking the microscopic motions of particles solves the problem [10].

In 1910, thermal transpiration and thermal creep, which are rarefied gas dynamic phenomena, were investigated by Knudsen [6, 11]. He applied longitude temperature gradient along the walls of the flow channel and observed that flow was driven from the cold end of a channel towards the hot end of the channel.

In recent decades, several experimental studies were done about influence of thermal transpiration and thermal creep on performance of micro devices [12, 13 and 14].

In this study, particle simulation of non-equilibrium flows in two geometries (simple microchannel, geometry like Knudsen compressor) with two different wall temperature distributions, namely, linear, and a stepwise profile have been investigated with a goal of deeper understanding of the relation between thermal transpiration and macroscopic flow characteristics.

II. GOVERNING EQUATION

The Boltzmann equation describes the flow in all the regimes, continuum, and continuum transition and free molecular. It is an integrodifferential equation proposed by Boltzmann in 1872. Limiting cases of this equation yield the continuum description, commonly based on the Euler or Navier–Stokes equations, at the extreme of the small mean free paths and the collisionless (or free molecular) flow at the extreme of large free paths [15]. The Boltzmann equation for a simple dilute gas is [3].

$$\frac{\partial}{\partial t}(nf)+c.\frac{\partial}{\partial r}(nf)+F.\frac{\partial}{\partial c}(nf)=\int_{-\infty}^{\infty}\int_{0}^{4\pi} n^2(f^*f_1^*)c_r\sigma d\Omega dc_1 \qquad (1)$$

Where (nf) is the product of number density (n) and the velocity distribution function (f). In this equation, (c) is the molecular velocity, (c_r), the relative molecular speed, (F), the external force per unit mass, the superscript (*) indicates post-collision values, (f) and (f_1) represent the distribution functions of two different types of molecules of class (c) and (c_1),

V. Azadeh Ranjbar is with the Dept. of Mechanical Engineering, University of Tehran, Tehran, Iran, (phone: 00989354419835; e-mail: v.azadehranjbar@gmail.com).

respectively, (σ), is the collision cross-section, (t) represents time, (r) the physical space, and (Ω) represents solid angle. The right-hand side of the Boltzmann equation is called the collision term and is the source of problems in finding a solution.

III. Flow Physics

As a simple physical example, consider two chambers divided by a thin aperture, one chamber has a high temperature (T_H) and pressure (P_H), and the other one has a lower temperature (T_L) and pressure (P_L). Thermal transpiration can take place through the aperture if the aperture area (A_a) is such that, ($A_a << \lambda$), where (λ) is the mean free path of the gas. The number of molecules crossing the aperture per unit time per unit area is ($n\bar{C}'/4$), where n is the number density and ($\bar{C}'$) is the mean thermal speed of the gas molecules. The number density, (n), is defined as (P/kT), where (P) represents pressure, k is the Boltzmann's constant, and (T) is the gas temperature. The mean thermal speed is given by ($\sqrt{8kT/\pi m}$), where (m) is the molecular mass. Therefore, there are ($A_a n_L \bar{C}_L'/4$), molecules per unit time passing through the aperture from cold to hot, and ($A_a n_H \bar{C}_H'/4$) molecules going from hot to cold. At steady state, the number flow of molecules from cold to hot minus the flow from hot to cold is equal to ($\dot{N}$) or :

$$\frac{n_L \bar{C}_L'}{4} A_a - \frac{n_H \bar{C}_H'}{4} A_a = \dot{N} \qquad (2)$$

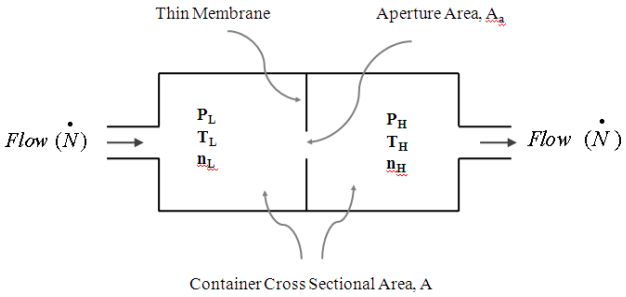

Fig. 1 Elementary single stage of a thermal transpiration compressor

Thus for ($\dot{N} = 0$), the pressure ratio (P_H=P_L) becomes:

$$\frac{p_H}{p_L} = \sqrt{\frac{T_H}{T_L}} \qquad (3)$$

For (P_H=P_L), the net number flow of molecules from cold to hot is:

$$\dot{N}_{\max} = A_a \frac{1}{\sqrt{2\pi mk}} p_L \left[T_H \sqrt{T_L} - T_L \sqrt{T_H} \right] / (T_H T_L) \qquad (4)$$

Hence, for (P_H) between (P_L) and ($P_L \sqrt{T_H / T_L}$), there will be both a pressure increase and a net flow, which are the requirements for a pump [16].

IV. Problem Definition

For modeling single stage of a thermal transpiration pump two different geometries are used.

In the first one, a simple two dimensional microchannel with an infinite width w is investigated, in this geometry the aperture is modeled by a microchannel which is superimposed with linear temperature gradients. Also two containers are substituted by two infinite containers. Therefore macroscopic characteristics of inlet and outlet flow (pressure, number density and temperature) are similar to characteristics of gas in low and high temperature chamber respectively. A schematic of the geometric configuration and notations are used throughout this study are shown in Fig. 2.

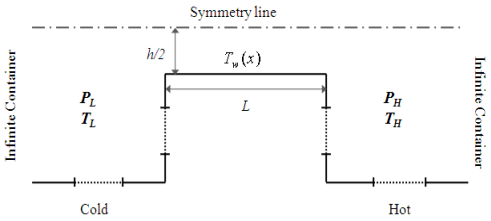

Fig. 2 The first geometry

The summary of cases that have been considered for this geometry is given in Table 1.

TABLE I
SUMMERY OF CASES STUDIED FOR THE FIRST GEOMETRY

	P_L=P_H (atm)	T_H (k)	< Kn <
Case1	0.125	1000	0.2-0.72
Case2	0.25	450	0.1-0.16
Case3	0.25	600	0.1-0.22
Case4	0.25	750	0.1-0.27
Case5	0.25	900	0.1-0.32
Case6	0.25	1000	0.1-0.36
Case7	0.5	600	0.05-0.1
Case8	0.5	1000	0.05-0.17
Case9	1.0	600	0.025-0.05
Case10	2.0	600	0.013-0.027
T_L=300 K			
L/h=5			

In the second one, for better understanding of thermal transpiration effects on macroscopic characteristics of flow instead of two infinite containers, two finite containers with length-to-height ratio H/L=5 and H/L=10 is used. Additionally, two different wall temperature distributions (linear and stepwise) are examined. This geometry has an infinite width w too. A schematic of the geometric configuration and notations are used throughout this study are shown in Fig. 3.

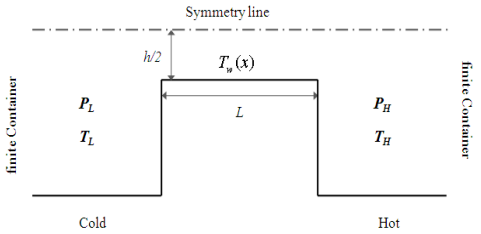

Fig. 3 The second geometry

The summary of cases that have been considered for this geometry is given in Table 2.

TABLE II
SUMMERY OF CASES STUDIED FOR THE SECOND GEOMETRY WITH LINEAR TEMPERATURE GRADIENT

	P_L=P_H (atm)	T_H (k)	Kn_L	< Kn_{Ch} <	Kn_H	L/h
Linear Temperature Distribution						
Case 11	4.0	600	0.04	0.2-0.4	0.08	5
Case 12	1.0	600	0.04	0.2-0.4	0.08	10
Case 13	1.0	600	0.1	0.21-0.43	0.21	5
Case 14	1.0	1000	0.1	0.21-0.71	0.36	5
Case 15	0.25	450	0.05	0.1-0.16	0.08	5
Case 16	0.25	600	0.05	0.1-0.22	0.1	5
Case 17	0.25	750	0.05	0.1-0.27	0.13	5
Case 18	0.25	900	0.05	0.1-0.32	0.16	5
Case 19	0.5	600	0.027	0.05-0.1	0.054	5
Case 20	1.0	600	0.013	0.025-0.05	0.027	5
Case 21	2.0	600	0.007	0.013-0.027	0.013	5
T_L=300 K						

TABLE III
SUMMERY OF CASES STUDIED FOR THE SECOND GEOMETRY WITH STEPWISE TEMPERATURE GRADIENT

	P_L=P_H (atm)	T_H (k)	Kn_L	< Kn_{Ch} <	Kn_H	L/h
Stepwise Temperature Distribution						
Case 22	4.0	600	0.04	0.2-0.4	0.08	5
Case 23	1.0	600	0.04	0.2-0.4	0.08	10
Case 24	1.0	600	0.1	0.21-0.43	0.21	5
Case 25	1.0	1000	0.1	0.21-0.71	0.36	5
Case 26	0.25	600	0.1	0.21-0.43	0.21	5
Case 27	0.25	1000	0.1	0.21-0.71	0.36	5
Case 28	0.25	450	0.05	0.1-0.16	0.08	5
Case 29	0.25	600	0.05	0.1-0.22	0.1	5
Case 30	0.25	750	0.05	0.1-0.27	0.13	5
Case 31	0.25	900	0.05	0.1-0.32	0.16	5
Case 32	0.5	600	0.027	0.05-0.1	0.054	5
Case 33	1.0	600	0.013	0.025-0.05	0.027	5
Case 34	2.0	600	0.007	0.013-0.027	0.013	5
T_L=300 K						

The gas is molecular Nitrogen in all simulations.

V. NUMERICAL SOLUTION

In this study, direct simulation Monte Carlo method as a particle simulation method is used. The core of the DSMC algorithm consists of four primary processes: move the particles, index and cross-reference the particles, simulate collisions, and sample the flow-field. The molecular motion and the intermolecular collisions are uncoupled over the small time interval– the discrete time-step.

In the first process, all the molecules are moved through distances appropriate to their velocity components and the discrete time-step. Appropriate action is taken if the molecule crosses boundaries representing solid surfaces, lines or surfaces of symmetry, or the outer boundary of the flow. As for the boundary conditions, the microscopic boundary conditions are specified by the behavior of the individual molecules according to the conservation laws, rather than in terms of the distribution function. Collisions with surfaces can be treated as being either fully specular, fully diffuse, or some combinations of the two.

The second DSMC process involves indexing and tracking the particles. A scheme for molecular referencing is the prerequisite for the next two steps: modeling the collisions and sampling the flow field.

The third step, simulating the collisions, is a probabilistic process that sets DSMC apart from deterministic simulation methods such as molecular dynamics. The probability of a collision between two molecules in a homogenous gas is proportional to the product of their relative speed and total collision cross-section.

The final process is sampling the macroscopic flow properties. The spatial coordinates and velocity components of molecules in a particular cell are used to calculate macroscopic quantities at the geometric centre of the cell.

The above-mentioned stages correspond to the solution of the Boltzmann equation (1) using the following splitting scheme within the short time-step [17].

$$\frac{\partial}{\partial t}(nf)+c.\frac{\partial}{\partial r}(nf)+F.\frac{\partial}{\partial c}(nf)=0 \qquad (5)$$

For the collision-less movement of molecules in the first step, and:

$$\frac{\partial}{\partial t}(nf)=\int_{-\infty}^{\infty}\int_{0}^{4\pi} n^2(f^*f_1^*)c_r\sigma\, d\Omega\, dc_1 \qquad (6)$$

Correspond to the molecular collisions in the third step. The DSMC procedure is explicit and time marching and it always produces a flow simulation that is unsteady. For an unsteady flow application, an ensemble of many computations may be assembled and averaged to obtain final results with an acceptable statistical accuracy.

To simulate a steady problem, each independent computation proceeds until a steady flow is established at a sufficiently large time, and the desired steady result is time average of all values calculated after reaching the steady state.

VI. Results And Discussion

In this study, in all cases, thermal transpiration flow is dominant and maximum net number flow is occurred in consequence of equality of pressure in cold and hot containers ($P_L = P_H$).

For computing net number flow, n_L and n_H are estimated by numerical solution and substituted in (2). Then for comparing numerical results with anticipated maximum net number flow from (4), Figs. 4 and 5 are exhibited.

In Fig. 4, dashdot line by applying cases 3, 7, 9, 10 and dash line by applying cases 16, 19, 20, 21 and dashdotdot line by applying cases 29, 32, 33, 34 are plotted. Also, temperature in hot container is assumed constant (T_H=600 K) and effect of pressure in amount of net number flow is investigated.

In Fig. 5, dashpot line by applying cases 2, 3, 4, 5, 6 and dash line by applying cases 15, 16, 17, 18 and dashdotdot line by applying cases 28, 29, 30, 31 are plotted. Pressure is constant ($P_L=P_H$=0.25 atm) and effect of temperature in hot container is investigated.

In both investigations, the results show that, in worst condition, net number flow magnitude predicted by the first geometry is about 15 percent lower than that calculated by (4), but for the second geometry, this difference is less than 5 percent. It is observed that results of the second geometry are more agreed with results from (4) than the first geometry.

Fig. 5 shows there is a summit for net number flow when T_H equal to infinite. This summit is a function of pressure, temperature in cold container, type of gas and cross section area of microchannel.

$$\begin{cases} P = \text{Constant} \\ T_H = \infty \end{cases} \Rightarrow \dot{N} = \frac{A_a p_L}{\sqrt{2\pi m k T_L}} \qquad (7)$$

A. Velocity and Pressure Fields in the First Geometry

In Fig. 6, it is illustrated how temperature gradient affect X-component of velocity in centerline. Constant values in cases 2,3,4,5 and 6 are $P_L=P_H$= 0.25 atm, T_L=300 K and T_H varies from 450 K to 1000 K. In all cases, it is observed that linear temperature gradient along the walls leads to linear increasing of velocity filed along the microchannel. Comparison of cases 2 to 6 shows higher temperature gradient produces higher velocity filed. In addition, the acceleration of particles is higher. It means the range of velocity variation in higher temperature gradient is more than one in lower temperature gradient.

In Fig. 7, the effect of pressure on X-component of velocity in centerline is showed. Pressure in containers varies from 0.125 atm to 0.5 atm for cases 1, 6, 8. Also T_L and T_H are 300 K and 1000 K, respectively. Influences of rarefied gas dynamic phenomena are more in higher Knudsen numbers. On the other hands, increase of pressure magnitude leads to decrease of Knudsen number. So it is expected X-component of velocity in centerline is decreased by increasing pressure and the results confirm it.

B. Velocity and Pressure Fields in the Second Geometry

In this part, for better comprehension of thermal transpiration effects, instead of two infinite containers, two finite containers are modeled. And the influences of length-to-height ratio, temperature gradient type and pressure on gas pressure and velocity filed are investigated.

In all cases which are illustrated in Figs. 8 and 9, the pressure equal to 1 atm and the influences of type and temperature gradient magnitude on gas velocity and pressure filed are investigated respectively.

Fig. 8 shows maximum X-component of velocity in centerline in both linear and stepwise temperature distribution, approximately equal and occurs at the end of microchannel, but velocity profiles along the microchannel are different. Also Fig. 8 illustrates temperature gradient magnitude has a great effect on velocity field magnitude.

Fig. 9 shows maximum pressure in stepwise temperature distribution is extremely higher than one in linear temperature distribution.

Knudsen numbers of all cases in Figs. 10 and 11 are equal. It is observed that changing of pressure does not have any influence in velocity and pressure field.

Figs. 12 and 13 illustrate that with equal Knudsen numbers if the length-to-height ratio enlarges, in both linear and stepwise temperature gradients, the velocity filed is affected and decreased.

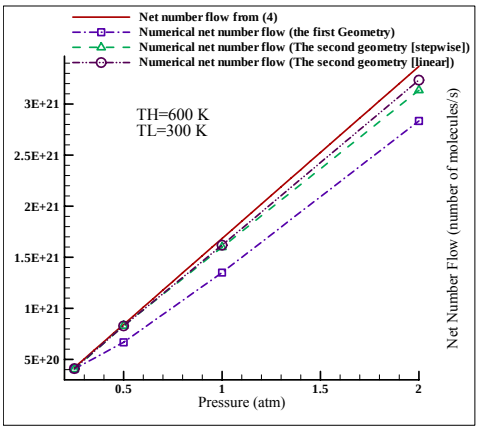

Fig. 4 Net number flow for different pressure

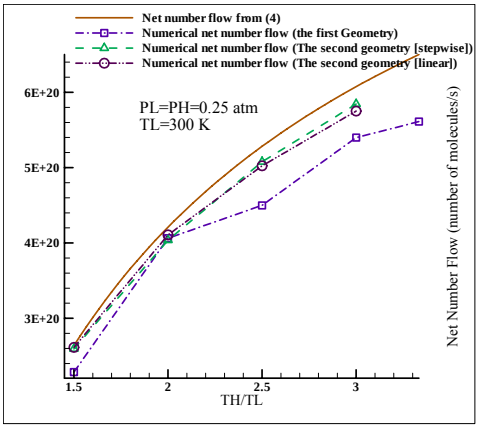

Fig. 5 Net number flow for different dimensionless Temperature

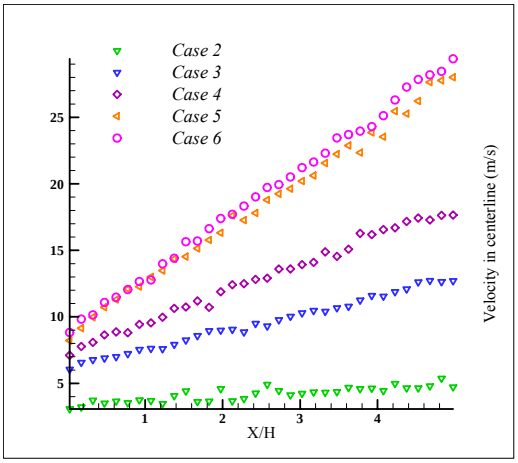

Fig. 6 X-component of velocity profile along the channel for different (T_H)

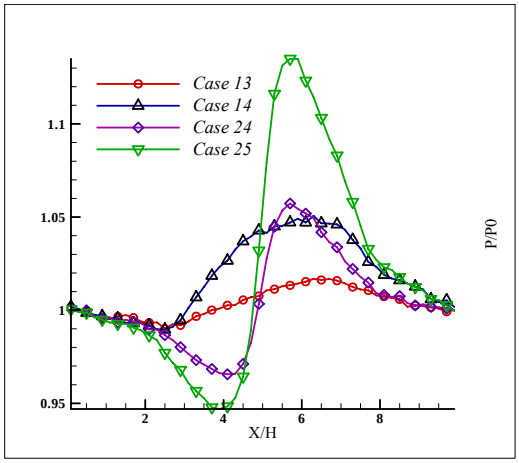

Fig. 9 Effect of different type and magnitude of temperature distributions on Pressure profile along the channel

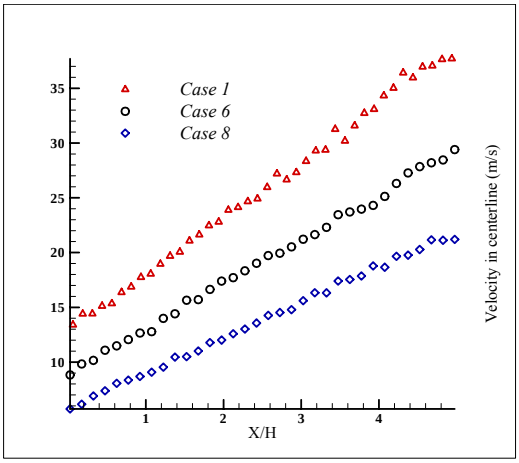

Fig. 7 X-component of velocity profile along the channel for different P_H=P_L

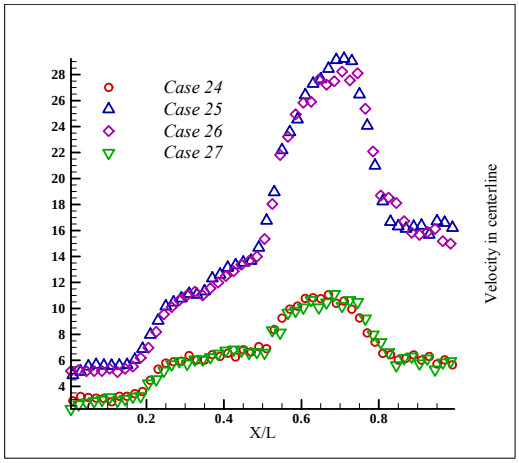

Fig. 10 Effect of different pressures on X-component of velocity profile along the channel

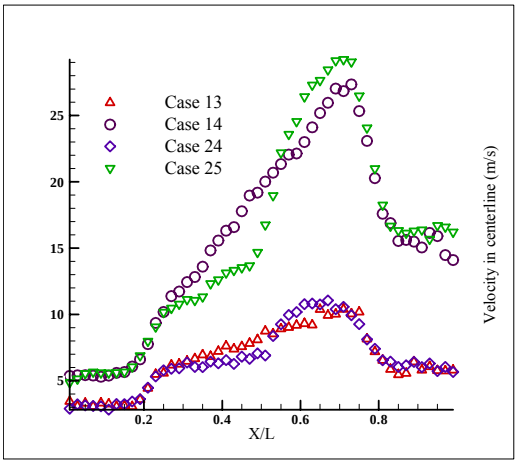

Fig. 8 Effect of different type and magnitude of temperature distributions on X-component of velocity profile along the channel

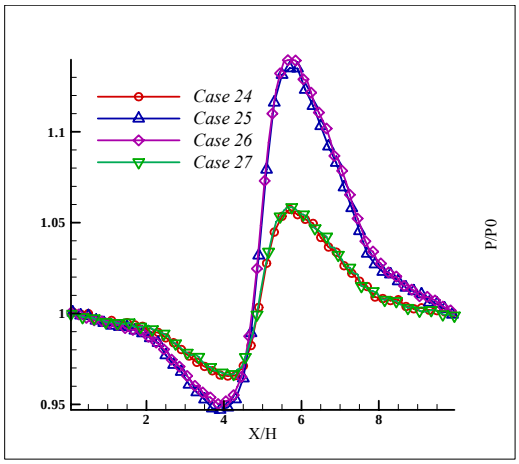

Fig. 11 Effect of different pressures on Pressure profile along the channel in different pressure

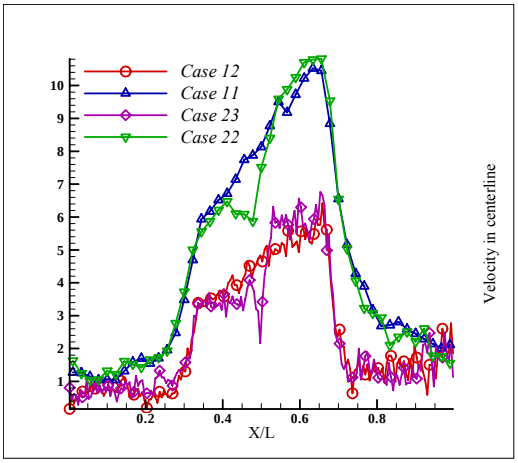

Fig. 12 Effect of length-to-height ratio on X-component of velocity profile along the channel

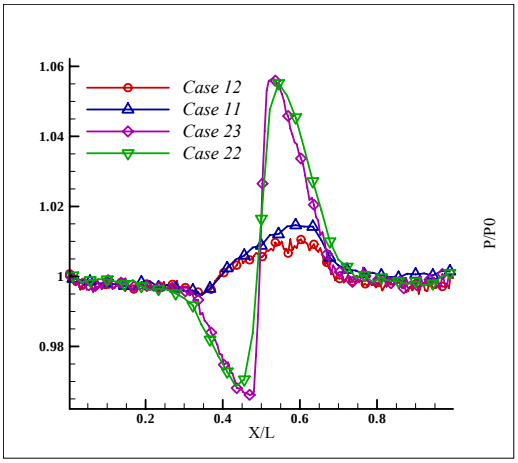

Fig. 13 Effect of length-to-height ratio on Pressure profile along the channel

VII. Conclusion

In this paper, direct simulation Mont Carlo method as a particle simulation method is applied to study about Thermal transpiration and thermal creep, which are rarefied gas dynamic phenomena. Results from the first geometry show that linear temperature gradients produce linear velocity fields and higher temperature gradients create higher velocity fields. Results from the second geometry illustrate that variables like temperature gradient and length-to-height ratio intensely affect macroscopic characteristics of flow. On the other hands, it is observed that in different situations with equal Knudsen numbers, changing of pressure does have no influence in macroscopic characteristics. It is observed that results of the second geometry have good agreement with analytical results. So for deeper understanding of rarefied gas dynamic phenomena in problem discussed, instead of a microchannel with infinite containers model, a microchannel with finite containers is suggested.

References

[1] G. E. Karniadakis, A. Beskok, N. Aluru, Microflows and Nanoflows: Fundamentals and Simulation, Springer, New York, 2005.
[2] C. Cai, I. D. Boyd, J. Fan, and F. V. Candler, "Direct simulation methods for low-speed microchannel flows", J. Thermophys. Heat Transfer 14(3)(2000), 368-378.
[3] Bird, G.A., 1976. Molecular Gas Dynamics. Clarendon Press, Oxford.
[4] G.A. Bird, Molecular Gas Dynamics and the Direct Simulations of Gas Flows, Oxford University Press (1994).
[5] Bird, G.A., 1998. Recent advances and current challenges for DSMC. Computers and Mathematics with Applications 35, 1–14.
[6] Knudsen, M. "Eine Revision der Gleichgewichtsbedingung der Gase. Thermische Molekularströmung." Ann. Phys. 31 (1910): 205.
[7] M.S, Ivanov, G.N, Markelov, S.F. Gimelshein, AIAA Paper 98-2669 (1998) .
[8] Liou, W.W., Fang, Y.C., 2000. Implicit boundary conditions for direct simulation Monte Carlo method in MEMS flow predictions. Computer Modeling in Engineering and Science 4, 119–128.
[9] Liou, W.W., Fang, Y.C., 2001. Heat transfer in microchannel devices using DSMC. Journal of Microelectromechanical Systems 10, 274–279.
[10] G. Pham-Van-Diep, D. Erwin, E. P. Muntz, *Scienc*e, 245, 624 (1989).
[11] Knudsen, M. "Thermischer Molekulardruck der Gase in Röhren." Ann. Phys. 33 (1910): 1435.
[12] Young, M., *Han, Y.L.*, Muntz, E.P., Shiflett, S. "Characterization and Optimization of a Radiantly Driven Multi-Stage Knudsen Compressor." 24th international Symposium on Rarefied Gas Dynamics. Bari, Italy, 2004.
[13] Young, M., Han, Y. L. "Aerogel as a Thermal Transpiration Membrane Material." 35th Annual SCCAVS Symposium, Anaheim, CA, 2002.
[14] E.P. Muntz, Y. Sone, K. Aoki, S. Vargo, M. Young, Performance analysis and optimization considerations for a Knudsen Compressor in transitional flow, J. Vac. Sci. Technol. A 20 (1) (2002) 214–224.
[15] C. Cercignani, *Rarefied gas dynamics. From basic concepts to actual calculations*, Cambridge University Press (2000).
[16] 12. Muntz, E.P. and Vargo, S.E. "Micro Scale Vacuum Pumps." The MEMS Handbook. Ed. G. Gad-el-Hak. CRC Press, 2002: 29_1-29_28.
[17] S. S. Sazhin, and V. V. Serikov, Rarefied gas flows: hydrodynamic versus Monte Carlo modeling, *Planetary Sp. Sci.*, **45**, 361–368 (1997).